24 to 28 GHz MMIC CLASS-J GaAs pHEMT POWER AMPLIFIER WITH NON-FOSTER MATCHING FOR 5G COMMUNICATION SYSTEMS

Charles Nwakanma Akwuruoha
Department of Electrical and Electronic Engineering,
Michael Okpara University of Agriculture, Umudike, Nigeria.
akwuruoha.charles@mouau.edu.ng

ABSTRACT

This paper presents 24 to 28 GHz MMIC (monolithic microwave integrated circuit) class-J GaAs pHEMT power amplifier with non-Foster matching for 5G communication systems. The power amplifier (PA) was designed with Keysight Advanced Design System (ADS) Software based on WIN semiconductor P10-10 GaAs pHEMT process technology with periphery of 150 µm and biased with drain supply voltage of 3 V at quiescent drain-to-source current of 3 mA. The transistors in the non-Foster circuit (NFC) were biased with drain supply voltage of 2 V with quiescent drain-to- source current of 2 mA. This puts the PA to NFC drain supply voltage scaling ratio at 1.5:1. The NFC produces the effective negative capacitance required to cancel out the power transistor input parasitic capacitance across the bandwidth in order to enhance PA efficiency, output power and gain. The PA has 4 GHz bandwidth as it operates from 24 to 28 GHz with center frequency of 26 GHz covering the proposed higher 5G frequency band of 24.5 to 27.5 GHz. Simulation results indicate that the PA with NFC has 36% drain efficiency, 26% power added efficiency (PAE), 16.2 dBm output power and transducer power gain of 5.2 dB at centre frequency of 26 GHz while the PA without NFC has 34% drain efficiency, 25% PAE, 15.6 dBm and transducer power gain of 4.6 dB at centre frequency of 26 GHz. The results indicate that the performance of the PA with NFC in terms of drain efficiency, power added efficiency, output power and transducer power gain from 24 to 28 GHz at centre frequency of 26 GHz increased by 2%, 1%, 0.6dBm and 0.6 dB respectively. This makes the PA suitable for application at higher 5G frequency band.

Keywords: Non-Foster, 5G, Negative capacitance, Wideband,Power amplifier**.**

I. INTRODUCTION

The ever-increasing demand for wireless communication applications has stimulated the desire for migration from 4G to 5G communication systems as proposed by Lin, (2018), Mumtaz *et al* (2018), Chen et al (2015) and Peral-Rosado *et al* (2018). The allocation of 5G frequency bands are categorized as lower and higher 5G bands namely 700 MHz, 3.4 to 3.8 GHz and 24.25 to 27.5 GHz respectively. In this work, the design frequency is 24 to 28 GHz which aims to cover the 5G high band of 24.25 to 27.5 GHz. The linear property of Class-J PA mode makes it suitable for 5G applications. Cripps (2006) proposed that Class-J PA mode mitigates the effects of transistor output capacitance on the fundamental load of PA by applying reactive termination to the fundamental load thereby changing it from resistive to reactive regime. Class-J PAs have also been reported by Wright *et al* (2009), Rezaei *et al* (2013), Tuffy *et al* (2011), Ma et al (2011), Mimis *et al* (2012), Anderson *et al* (2012), Park *et al* (2015), Jain *et al* (2013). However, the reported Class-J PAs, did not discuss the need to mitigate the effects of transistor input parasitic capacitance with negative capacitance from 24 to 26 GHz as proposed in this paper. In this work, NFC has been used in the PA input matching network to generate the negative capacitance required to cancel out the power transistor input parasitic capacitance in order to enhance PA performance and sustain the wide bandwidth. Non-Foster circuit violates reactance theorem (Akwuruoha *et al*., 2017; Muller and Lucyszyn, 2015; Sussman-Fort and Rudish, 2009) reported that NFC has negative reactance versus frequency slope and reflection coefficient which moves in counter-clockwise direction with respect to frequency on Smith chart. Elfrgani and Rojas (2015) and Larky (1957) proposed that Non-Foster circuits are classified as negative impedance converters (NIC) and negative impedance inverters (NII). The use of active devices in NIC design was first proposed by Linvill (1953) whereby the NIC was described as active

two-port network such that the input current equals the output current and the input voltage equals the negative of the output voltage while having input impedance which is equal to the reciprocal of the output impedance. The NIC was classified as open circuit stable (OCS) and short circuit stable (SCS). In this paper, open circuit stable NIC is proposed. Non-Foster circuits find application in many microwave devices ranging from Antennas: Haskou *et al* (2017), Jacob *et al* (2014) to power amplifiers: Lee *et al* (2015), Ghadiri and Moez (2010) and Ledezma (2015), Akwuruoha and Hu (2017). To the best of the author's knowledge, this is the first reported use of NFC to enhance the drain efficiency, PAE, output power and transducer power gain of wideband Class-J PA from 24 to 28 GHz for 5G applications. This paper is structured as follows. Section II discusses Class-J theory and Non-Foster Circuit theory. Section III discusses materials and methods. Section IV discusses non-Foster matching circuit design and PA design as well as simulation results. Section V concludes the paper.

II. THEORY

A. Class-J Theory

Wright *et al* (2009) reported that in Class-J PA mode, the application of reactive termination to the fundamental load results in higher order even harmonics than second harmonic becoming non-existent while the third harmonic is considered shorted out. Rezai *et al* (2013) reported that there is 45^o phase shift between the drain current and voltage of Class-J power transistor. The drain current and voltage are sine waves with even harmonics such that drain current and voltage waveforms with phase angle Ø are given by

$$I_{DD}(\emptyset) = \frac{I_{D,max}}{\pi} + \frac{I_{D,max}}{2cos\pi} + \frac{2I_{D,max}}{3cos2\emptyset} \quad (1)$$

where $I_{D,\,max}$ is the transistor peak current.

$$V_{DD}(\emptyset) = (V_D - V_{knee})\left[\cos(\emptyset) - \sin(\emptyset) + \frac{\sin(2\emptyset)}{2}\right] \quad (2)$$

where V_D and V_{knee} are the DC drain current and transistor knee voltage respectively.

According to Wright *et a*l (2009), the fundamental and second harmonic components of impedance denoted by Z_{fo} and Z_{2fo} are dependent on the optimum load resistance (R_{opt}) given by

$$R_{opt} = \frac{V_D}{\left({}^{I_{D,max}}/_{2}\right)} \quad (3)$$

$$Z_{f0} = R_{opt} + jR_{opt} \quad (4)$$

$$Z_{2f0} = 0 - j\left(\frac{3\pi}{8}\right)R_{opt} \quad (5)$$

The shorted third harmonic component of impedance is given by

$$Z_{3f0} = 0 \quad (6)$$

B. Non-Foster Circuit Theory

Non-Foster matched circuits have reflection coefficient which move in a counter-clockwise direction with respect to frequency on a smith chart. Muller and Lucyszyn (2015) reported that the relationship between reactance (X) and susceptance (B) of NFC denoted by X_{NFC} and B_{NFC} and its angular frequency (ω) are given by the derivatives:

$$\frac{dX_{NFC}}{d\omega} < 0 \quad (7)$$

$$\frac{dB_{NFC}}{d\omega} < 0 \quad (8)$$

III. MATERIALS AND METHODS

A. Materials

The Materials are Keysight Advanced Design System (ADS) software and WIN Semiconductor P10-10 GaAs pHEMT process design kit.

B. Methods

i) Non-Foster Matching Circuit design

The non-Foster matching circuit was designed with two WIN P10-10 process GaAs pHEMTs with periphery of 150 µm each biased with drain supply voltage of 2V with quiescent drain-to-source current of 2mA as shown by the DC bias points in Figure 1. The values of the lumped components used in the NFC design are shown in the NFC schematic circuit in Figure 2. The magnitude and imaginary part of input impedance (Z_{in}) showing the negative reactance versus frequency characteristics of the NFC is shown in Figure 3. The effective negative capacitance of the NFC across the 4 GHz bandwidth from 24 to 28 GHz is shown in Figure 4. The NFC effective negative capacitance ranges from -1.2 to -1.8 pF. The effective capacitance at 26 GHz center frequency stood at -1.3 pF.

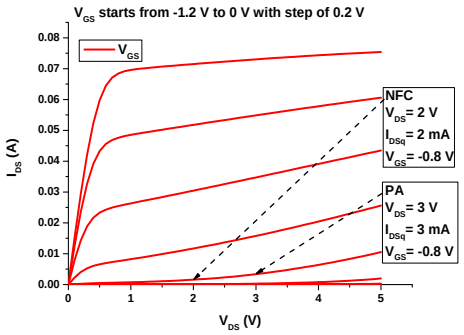

Figure 1. DC I-V characteristics bias points

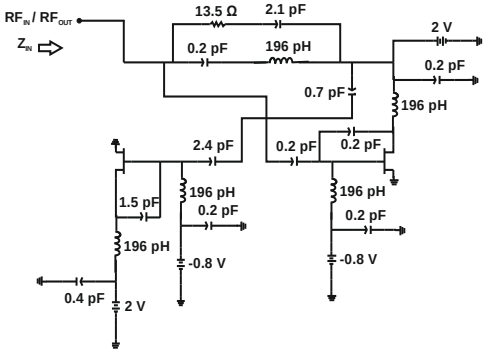

Figure 2. NFC schematic circuit

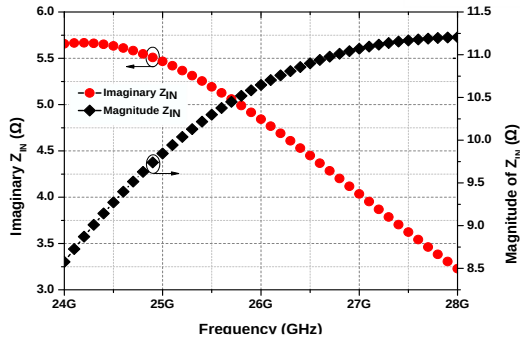

Figure 3. Magnitude and Imaginary part of input impedance

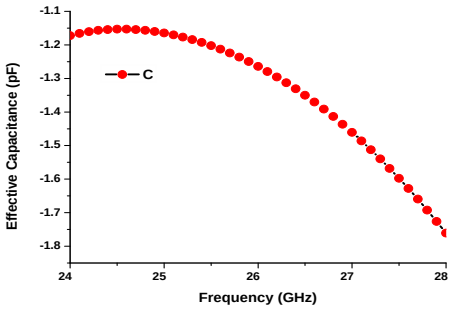

Figure 4. Effective negative capacitance

ii) PA Design

The PA was designed based on WIN P10-10 GaAs pHEMT process with periphery of 150 µm biased with drain supply voltage of 3V at quiescent drain-to-source current of 3mA.The PA circuit consists of distributed transmission lines as well as capacitors, inductors and resistors as shown in Figure 5. Harmonic source and load pull simulations were used to obtain the source and load impedances respectively required to synthesize the input and output matching networks for maximum power at 26 GHz center frequency. The NFC forms part of the input matching network and generates the effective negative capacitance required to cancel out the power transistor input parasitic capacitance. Stability resistor has been added to the input matching network to enhance

the PA stability and complement the input/output stability networks. This is aimed at forestalling the oscillations that could result from the NFC circuit. The PA was terminated with 50 Ω source and load impedance.

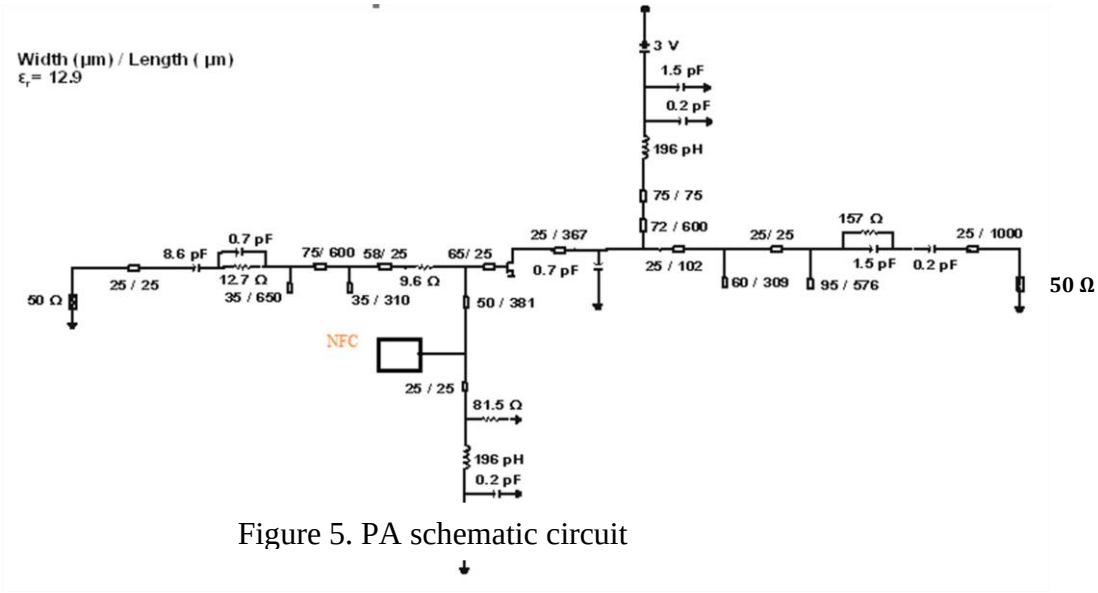

Figure 5. PA schematic circuit

IV RESULTS AND DISCUSSION

The result of the PA design is discussed in accordance with small and large signal simulations.

1) Small signal simulation

Small signal s-parameter simulation was carried out on the PA to determine the S_{21} values of the PA with NFC (denoted by PA_w_NFC) and the PA without NFC (denoted by PA_wo_NFC) as well as stability. The PA stability involving stability factor and measure indicates that the PA is unconditionally stable as shown in Figure 6. Further stability test using Nyquist criterion also indicates that the PA is stable as the input return loss did not encircle the origin in the polar plot in Figure 7. This is because according to Nagarkoti et al (2014), the encirclement of the origin in the Nyquist plot indicates instability. S_{21} result of the PA with and without NFC indicates that the PA with NFC has S_{21} of 5.4 dB while the one without NFC has S_{21} of 3.6 dB at 26 GHz center frequency as shown in Figure 8. This indicates 1.8 dB increase in small signal gain for the PA with NFC.

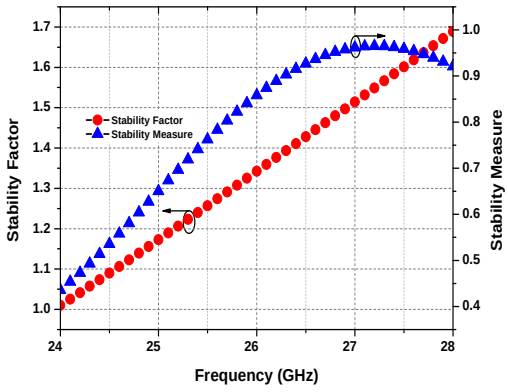

Figure 6. Stability Factor and Stability Measure

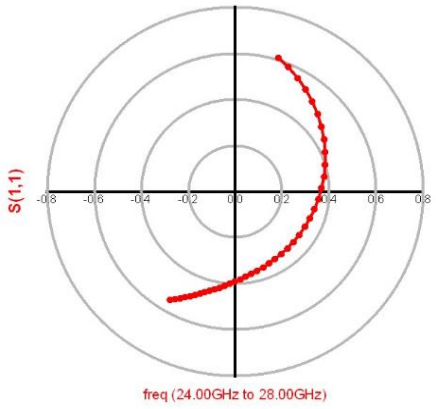

Figure 7. Nyquist stability diagram from 24 GHz to 28 GHz

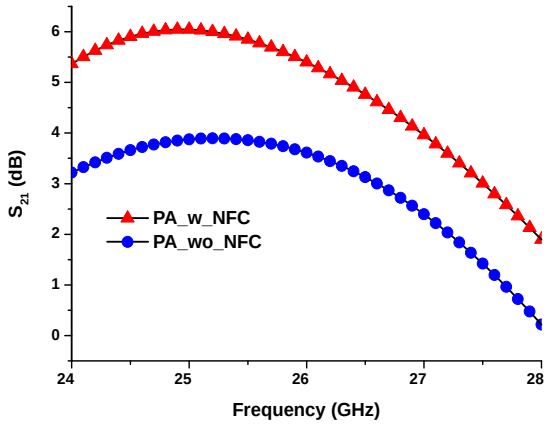

Figure 8. Small signal gain (S_{21})

2) Large Signal Simulation result

One-tone harmonic balance simulation was carried out on the PA with and without NFC. The input power was swept from 0 to 11 dBm at 26 GHz as shown in Figures 9 and 10. At 26 GHz center frequency and input power of 11dBm, the PA with NFC has 36% drain efficiency, 26% PAE, 16.2 dBm output power and 5.2 dB gain while the PA without NFC has 34% drain efficiency, 25% PAE, 15.6 dBm output power and 4.6 dB gain. This result indicates that the PA with NFC has higher drain efficiency, PAE, output power and power gain than the PA without NFC. This represents 2% increase in drain efficiency, 1% increase in PAE, 0.8 dBm increase in output power and 0.6 dB increase in power gain for the PA with NFC. This is a significant increase in PA performance at GHz frequency where the effects of parasitic capacitances are more pronounced.

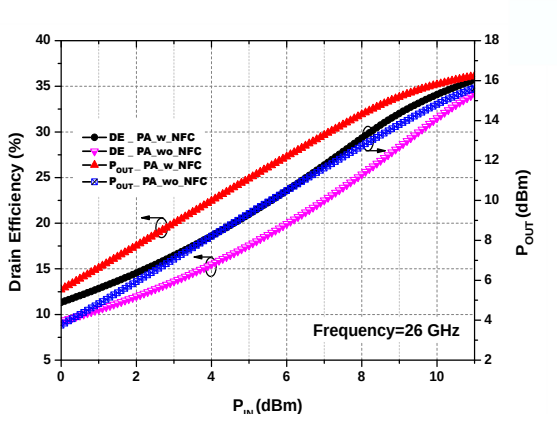

Figure 9. Drain Efficiency and output power versus input power

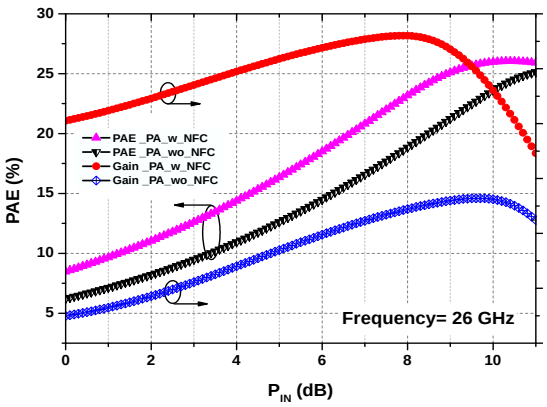

Figure 10. PAE and gain versus input power

V. CONCLUSION

A 24 to 28 GHz MMIC Class-J GaAs pHEMT power amplifier with non-Foster matching for 5G communication system has been proposed, designed and simulated. The simulation results show that the PA with non-Foster matching has better performance in terms of efficiency, output power and power gain than the PA without non-Foster matching. The PA will be suitable for deployment in the 5G frequency of 24.25 to 27.5 GHz.

ACKNOWLEDGMENT

The author is thankful to WIN Semiconductors for providing the model used in this work.

REFERENCES

Akwuruoha, C, N., Hu, Z. & Licea, Y. J. (2017). Microstrip non-foster circuit high efficiency high power class-J GaN HEMT amplifier, IEEE Conference on Microwaves, Antennas, Communications and Electronic Systems, Tel-Aviv, Israel, 1-4.

Akwuruoha, C. N. and Hu, Z. (2017). 64 to 70 GHz Microstrip Non-Foster Circuit Class-J GaAs pHEMT power amplifier, 25th Telecommunication Forum, Belgrade, Serbia, 1-4.

Anderson, C. M. et al (2012). Theory and Design of Class-J Power Amplifiers with Dynamic Load Modulation, *IEEE Transactions on Microwave Theory and Techniques*, 60 (8), 2562-2570.

Chen, S., Sun, S., Wang, Y., Xiao, G. & Tamrakar, R. (2015). A comprehensive survey of TDD-SCDMA 3G to TD-LTE, A 4G and 5G directions, *China Communications*, 12 (2), 40-60.

Cripps, S. C. (2006). RF Power Amplifiers for Wireless Communications, Second edition, Artech House, 68-89.

Elfrgani, E. M. & Rojas, R. G. (2015). Successful Realization of Non-Foster Circuits for Wide-Band Antenna Applications, IEEE MTT-S International Microwave Symposium, Phoenix, AZ, USA,1-4.

Ghadiri, A. and Moez, K. (2010). Gain-Enhanced Distributed Amplifier using Negative Capacitance, *IEEE Transactions on Circuits and Systems*, 57 (11), 2834-2843.

Haskou, A., Lemurs, D., Collardey, S., & Sharaiha, A. (2017). A non-foster circuit design for antenna miniaturization, International Symposium on Antennas and Propagation, Okinawa, Japan, 286-287.

Jacob, M. M., Long, J., & Sievenpiper, D. F. (2014). Non-Foster Loaded Parasitic Array for Broadband Steerable Patterns, *IEEE Transactions on Antenna and Propagation*, 62 (12), 6081-6090.

Jain, A., Hannurkar, P. R., Pathak, S. K., Sharma, D. K., & Gupta, A. K. (2013). Investigation of class-J high-power solid state RF amplifier, *IET Microwave Antennas Propagation* 7(8), 686-692.

Larky, A. I. (1957). Negative-Impedance Converters, *IRE Transactions on Circuit Theory*, 124-131.

Ledezma, L. M. (2015). Doherty power amplifier with lumped non-foster impedance inverter, Symposium on Wireless and Microwave Circuit and Systems, Waco, Texas USA, 1-4.

Lee, S., Park, H., Kim, J., & Kwon, Y. (2015). A 6-18 GHz GaN pHEMT Power Amplifier Using Non-Foster matching, IEEE MTT-S International Microwave Symposium, Phoenix, AZ, USA, 1-4.

Lin, J. C. (2018). Synchronization Requirements for 5G: An Overview of Standards and Specializations for Cellular Networks, *IEEE Vehicular Technology Magazine*, 13 (3), 91-99.

Linvill, J. G. (1953). Transistor Negative–Impedance Converters, *Proceedings of the IRE*, 725-729.

Ma, R., Goswami, S., Yamanaka, K., & Komatsuzuki, Y. (2011). A 40-dBm high voltage broadband GaN Class-J power amplifier for PoE micro-basestations, *IEEE MTT-S International Microwave Symposium Digest*, 1-4.

Mimis, K., Moris, K. A., Bensmida, S., & Mc Geehan, J.P. (2012). Multichannel and Wideband Power Amplifier Design Methodology for 4G Communication Systems Based on Class-J operation, *IEEE Transactions on Microwave Theory and Techniques*, 60 (12), 3778-3786.

Muller, A. A. & Lucyszyn, S. (2015). Properties of purely reactive Foster and non-Foster passive networks, *Electronic Letters*, 51 (23), 1882-1884.

Mumtaz, S., Bo, A., Al-Dulaimi, A. A., & Tsang, K. F. (2018). Guest Editorial 5G and Beyond Mobile Technologies and Applications for Industrial IoT (IIoT), *IEEE Transactions on Industrial Informatics*, 14 (6), 2588-2591.

Nagarkoti, D. S., Rajah, K. Z., & Hao, Y. (2014). Design and Stability of Negative Impedance Circuits for Non-Foster Matching of a Monopole Antenna, 8th European Conference on Antennas and Propagation, The Hague, Netherlands, 2707-2709.

Park, S., Woo, J., Kim, U., & Kwon, Y. W. (2015). Broadband CMOS Stacked RF Power Amplifier Using Reconfigurable Interstage Network for Wideband Envelope Tracking, *IEEE Transactions on Microwave Theory and Techniques*, 63(4), 1174-1185.

Peral-Rosado, J. A., Raulefa, R., Lopez-Salcedo, J. A., & Seco-Granados, G. (2018). *IEEE Communications Surveys and Tutorials*, 1(2), 1124-1148.

Rezaei, S., Belostotski, L., Ghannouchi, F. M., & Aflaki, P. (2013). Integrated Design of a Class-J Power Amplifier, *IEEE Transactions on Microwave Theory and Techniques*, 61(4), 1639-1648.

Sussman-Fort, S. E., & Rudish, R. M. (2009). Non-Foster Impedance Matching of Electrically-Small Antennas, *IEEE Transactions on Antennas and Propagation*, 57 (8), 2230-2241.

Tuffy, N., Zhu, A., & Brazil, T. J. (2011). Class-J RF power amplifier with wideband harmonic suppression, *IEEE MTT-S International Microwave Symposium Digest*, 1-4.

Wright, P., Lees, J., Benedikt, J., Tasker, P. J., & Cripps, S. C. (2009). A Methodology for Realizing High Efficiency Class-J in a Linear and Broadband PA. *IEEE Transactions on Microwave Theory Techniques*, 57 (12), 3196-3204.